

# Characterization and Preparation of New Multiwall Carbon Nanotube/Conducting Polymer Composites by *In Situ* Polymerization

Ali Md Showkat,<sup>1</sup> Kwang-Pill Lee,<sup>1</sup> Anantha Iyengar Gopalan,<sup>1,2</sup> Sang-Ho Kim,<sup>1</sup> Seong-Ho Choi,<sup>3</sup> Sang-Ho Sohn<sup>4</sup>

<sup>1</sup>Department of Chemistry Graduate School, Kyungpook National University, Daegu 702-701, South Korea

<sup>2</sup>Department of Industrial Chemistry, Alagappa University, Karaikudi 630003, Tamil Nadu, India

<sup>3</sup>Department of Chemistry, Hannam University, Daejeon 306-791, South Korea

<sup>4</sup>Department of Physics, Graduate School, Kyungpook National University, Daegu 702-701, South Korea

Received 3 June 2005; accepted 1 October 2005

DOI 10.1002/app.23359

Publication online in Wiley InterScience (www.interscience.wiley.com).

**ABSTRACT:** Composites based on poly(diphenyl amine) (PDPA) and multiwall carbon nanotubes (MWNTs) were prepared by chemical oxidative polymerization through two different approaches: *in situ* polymerization and intimate mixing. In *in situ* polymerization, DPA was polymerized in the presence of dispersed MWNTs in sulfuric acid medium for different molar composition ratios of MWNT and DPA. Intimate mixing of synthesized PDPA with MWNT was also used for the preparation of PDPA/MWNT composites. Transmission electron microscopy revealed that the diameter of the tubular structure for the composite was 10–20 nm higher than the diameter of pure MWNT. Scanning electron microscopy provided evidence for the differences in the morphology between the MWNTs and the composites. Raman and Fourier transform IR (FTIR) spectroscopy, thermogravimetric analysis, X-ray diffraction, and UV–visible spec-

troscopy were used to characterize the composites and reveal the differences in the molecular level interactions between the components in the composites. The Raman and FTIR spectral results revealed doping-type molecular interactions and coordinate covalent-type interactions between MWNT and PDPA in the composite prepared by *in situ* polymerization and intimate mixing, respectively. The backbone structure of PDPA in the composite decomposed at a higher temperature (>340°C) than the pristine PDPA (~300°C). This behavior also favored the molecular level interactions between MWNT and PDPA in the composite. © 2006 Wiley Periodicals, Inc. *J Appl Polym Sci* 101: 3721–3729, 2006

**Key words:** carbon nanotubes; poly(diphenyl amine); polymerization; conducting polymer; nanocomposites

## INTRODUCTION

Carbon nanotubes (CNTs) with their unique electronic and mechanical properties<sup>1,2</sup> not only represent suitable model structures for sophisticated research but also form the basis of preparing a new class of advanced materials for applications in nanotube reinforced materials, nanoelectronic devices, field emitters, and so forth.<sup>3–8</sup> Preparation of a CNT/polymer composite is an effective approach to produce tailor-made synergic contributory properties of the two components in the composite. CNT/polymer nanocomposites were prepared as nanostructural and functional materials for targeted applications.<sup>9–11</sup> CNTs were used as conductive fillers in CNT/polymer composites with poly(3-octyl thiophene) or poly(phenylene vinylene) as the polymeric matrix.<sup>12,13</sup>

A few conducting polymer/CNT composites have been prepared. Among the conducting polymers, polyaniline (PANI) has received greater attention because of its unique advantages like environmental stability, electrochemical switchability, and durability.<sup>14</sup> Studies on CNT/PANI composites have been reported.<sup>15–20</sup> Thus, it has become important to understand the physical/chemical interactions between the CNT and conducting polymer. There can be molecular level interactions between the CNT and conducting polymer and this can ultimately decide the properties of the composites. Ultimately, the properties of the composites depend on the method of preparation of the composites.

There are two general methods for the preparation of composites comprising CNTs and conducting polymers. One involves the direct mixing of the two components and the other one utilize chemical synthesis. The former method aims for intimate mixing of the two components and mostly involves an undoped conducting polymer to mix with the CNTs. The latter method consists of performing the polymerization of the respective monomer in the presence of added

Correspondence to: K.-P. Lee (kplee@knu.ac.kr).

Contract grant sponsor: Korean Research Foundation; contract grant number: KRF-2004-005-00009.

CNTs. Here, the conditions of polymerization can also contribute to the structural modifications of both components. Hence, a comparative study on the preparation and characterization of a CNT/conducting polymer composite would reveal the subtle differences in the properties between the composites prepared through these two different approaches.

Poly(diphenyl amine) (PDPA), an *N*-aryl substituted aniline, has been found to show many properties that are different from PANI and other *N*-substituted aniline derivatives.<sup>20–22</sup> The utility of PDPA as an amperometric sensor,<sup>23,24</sup> as a sorbent for solid-phase extraction,<sup>25</sup> as a sensor for alcohol,<sup>26</sup> as an electrochromic material,<sup>27</sup> for modified electrode formation,<sup>28</sup> and as a pH sensor<sup>29</sup> have been established. Such studies have revealed that PDPA can form an effective alternative to PANI, and PDPA is known to have better solubility than PANI.<sup>30</sup> Recent studies<sup>31,32</sup> have attempted to incorporate newer properties into PDPA by grafting a nonconducting polymer onto its backbone. In fact, this creates the possibility of the creation of new polymeric materials with interesting characteristics. Studies on the preparation and characterization of a composite of CNT with PDPA have not reported thus far.

In the present work, we prepared composites of multiwall carbon nanotubes (MWNTs) with PDPA. The composites were produced by mixing PDPA with MWNTs and by performing *in situ* polymerization of DPA in the presence of MWNTs. Molecular level interactions between the MWNTs and PDPA were analyzed. The composites were characterized for the differences in morphology, structure, and optical and thermal properties between the composites prepared through different methods.

## EXPERIMENTAL

### Materials

DPA (E. Merck) was doubly recrystallized from petroleum ether. The other chemicals in the study were also E. Merck products. MWNT samples were purified and used. The samples were suspended in 4M HCl solution, ultrasonicated for 6 h, centrifuged, filtered, and dried before use.

### Preparation of MWNT/PDPA nanocomposites

The composites were prepared by two different methods: intimate mixing of neutral PDPA with MWNT (method 1, IM) and *in situ* polymerization of DPA in the presence of MWNT (method 2, IP).

Intimate mixing of PDPA and neutral PDPA

*Preparation of neutral pdpa.* A solution of ammonium peroxydisulfate (20 mM) was added dropwise to a

stirred solution of DPA (40 mM) in 4M aqueous H<sub>2</sub>SO<sub>4</sub> at 4°C, and the stirring was continued for 2 h. The initial color of the medium was purple and it then changed to green. The green-colored precipitate (doped PDPA) was filtered out of the medium, washed several times with doubly distilled water until the filtrate was colorless, and dried. Neutralized PDPA was obtained by treating the doped PDPA with aqueous NH<sub>3</sub> solution for 24 h. The blue-colored PDPA (neutralized) was washed with distilled water and dried. Intimate mixing.

Composites were prepared by mixing a solution of neutral PDPA in chloroform with an appropriate amount of MWNT followed by subsequent evaporation of the solvent. Composite samples IM1 and IM2 were prepared by the addition of 0.003 and 0.03 g of MWNT, respectively, to a solution of neutral PDPA (0.1 g) in 5 mL of chloroform.

### *In situ* polymerization of DPA in presence of MWNT

Composite samples IP1 and IP2 were prepared by maintaining 0.007 and 0.07 g of MWNT in the polymerization conditions, respectively. In a typical experiment, 0.007 g of MWNTs were added to a solution of DPA in 4M H<sub>2</sub>SO<sub>4</sub> (40 mM). The mixture was cooled to 4°C using a freezing mixture. A precooled (4°C) solution of ammonium peroxydisulfate (0.1M) in 4M H<sub>2</sub>SO<sub>4</sub> was added dropwise to the mixture with stirring. The resulting green precipitate (acid-doped composite) was filtered through a sintered glass crucible and washed with 4M H<sub>2</sub>SO<sub>4</sub> until the filtrate became colorless. The acid-doped composites were then dried under a dynamic vacuum at room temperature. Blue-colored neutral composite was obtained when treating the acid-doped composites (IP1 and IP2) with aqueous ammonia. The neutral composites thus obtained from IP1 and IP2 were designated as IP1N and IP2N, respectively.

### Characterization

The Fourier transform IR (FTIR) spectra of the composites were recorded using a Bruker IFS 66v FTIR spectrophotometer in the 500–4000 cm<sup>-1</sup> region using KBr pellets. UV-visible spectra were recorded in DMF using a Shimadzu UV-visible spectrophotometer. Thermogravimetric analysis was performed using a TA Instruments 2950 Hi-Res apparatus at a heating rate of 10°C/min under a nitrogen atmosphere. The powder X-ray diffraction (XRD) patterns of the composites were recorded in the 2θ region on a Rigaku diffractometer using nickel-filtered Cu Kα radiation. The morphology of the samples was examined by scanning electron microscopy (SEM, Hitachi S-4200) and transmission electron microscopy (TEM, JEOL JEM-2000EX). For recording the Raman spectrum, the

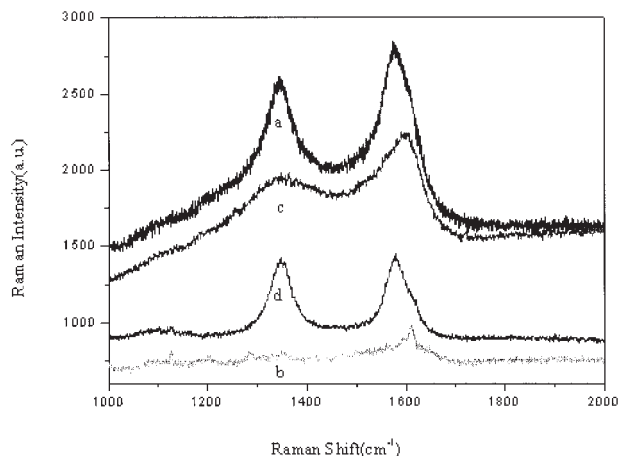


**Figure 1** Raman spectra of the neutral composite of MWNT and PDPA prepared by intimate mixing (IM1, spectrum a), the composite prepared by *in situ* polymerization (IP1N, spectrum b), neutralized PDPA (spectrum c), and pure MWNT (spectrum d).

sample was sealed in a pyrex glass capillary sample tube with an internal diameter of 2 mm, which was mounted in a sample illuminator. The Raman spectrum was recorded in the 1000–2000  $\text{cm}^{-1}$  region using a HORIBA Jobin Yvon HR800 Raman spectrophotometer with 514-nm radiation from an  $\text{Ar}^+$  ion laser excitation source. The conductivity of the samples was determined by the two-probe method using pressed pellets.

## RESULTS AND DISCUSSION

### Raman spectroscopy

Figure 1 displays the Raman spectra of the composites prepared by intimate mixing of neutral PDPA and MWNT and *in situ* polymerization of DPA in the presence of MWNT. The spectra of the parent MWNT and neutral PDPA are also presented (Fig. 1). A comparison of the spectra (Fig. 1) clarifies that there are differences in the molecular level interactions between the groups present in the MWNT and PDPA for the composites prepared by the two methods. Raman spectroscopy was previously used to show the interactions between CNTs and the polymer structure.<sup>20,31–35</sup> The bands that appear at around 1350 and 1580  $\text{cm}^{-1}$  for pure MWNT show distinct variations in intensities and positions when made into composites with PDPA through the two methods. We envisage that such variations in the band positions may arise as a result of the differences in molecular level interactions between the groups in the PDPA and MWNTs.

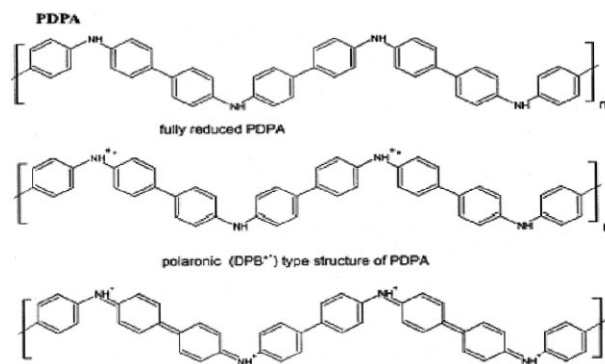
Composites of PANI and CNTs prepared by different methods have been described as having differences in molecular level interactions between the components.<sup>33</sup> For the PANI–CNT composites prepared

with intimate mixing, polymer functionalized CNTs have been reported to result through the formation of new C–N covalent bonds. In contrast, the composites prepared by *in situ* polymerization have interactions similar to doping of PANI with CNTs.<sup>34</sup>

The Raman band appearing at around 1580  $\text{cm}^{-1}$  was assigned to the  $E_{2g}$  vibration of the infinite crystal and was considered to be associated with a graphitic carbon with an  $sp^2$  electronic configuration. Polycrystalline graphite showed a distinct peak at 1350  $\text{cm}^{-1}$  that was due to the  $A_{1g}$  mode, which was attributed to a diamondlike carbon with an  $sp^3$  configuration. In Figure 1 it is evident that the bands at around 1580 and 1350  $\text{cm}^{-1}$  for pure MWNT show variations when made into a composite by the two methods. The composite for IM1 has a significant increase in intensities for both bands, with a shift to lower wavenumbers. Conversely, the composite IP1N shows a drastic decrease in peak intensities with a shift toward higher wavenumbers. These differences can be ascribed to the associated differences in molecular interactions between PDPA and MWNT in these two composites. It is important to note that the vibrational modes of the composites comprise the sum of the contributions from MWNTs or nanotube fragments and PDPA/MWNT (whole fragment) composites. This is inferred from a comparison of the Raman bands of neutral PDPA (Fig. 1). Although we could not get a clear picture for the microstructure in these two composites from the Raman spectra, it is pertinent to note that the interactions of MWNTs with PDPA can be from any one of the probable redox sites in PDPA (Scheme 1). We believe that MWNT can interact with any of these redox sites in PDPA while forming the composites with PDPA.

### FTIR spectroscopy

The FTIR spectra (Figs. 2, 3) provide further convincing evidence for the differences in the molecular level interactions in the components of the composites pro-



**Scheme 1** The structure of PDPA in different redox states.

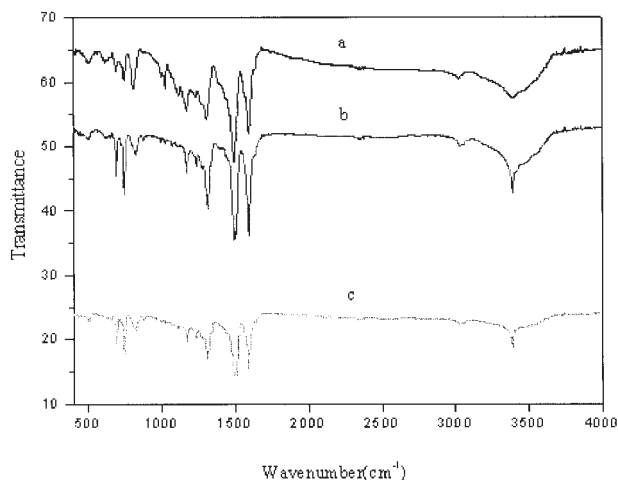


**Figure 2** FTIR spectra of the neutralized composite prepared by intimate mixing (IM1, spectrum a), the neutral composite prepared by *in situ* polymerization (IP1N, spectrum b), and neutral PDPA (spectrum c).

duced by the two procedures (intimate mixing and intimate polymerization). To understand the differences in the spectral characteristics of the composites, the bands in the FTIR spectrum of neutral PDPA are assigned and compared. The main absorption bands in neutral PDPA situated around 810, 1170, 1320, 1500, and 1600  $\text{cm}^{-1}$  are assigned to the following vibrations: bending C—H (out of plane) on the benzene ring (B), bending of the C—H (in plane) vibration of the N=quinoid ring (Q=N), stretching of  $\text{C}_{\text{aromatic}}-\text{N}$ , stretching of the N—B—N ring, and stretching of N=Q=N, respectively. The bands around 1600 and 1500  $\text{cm}^{-1}$  show the variations in intensities between the composites prepared by the two methods. The higher frequency band ( $\sim 1600 \text{ cm}^{-1}$ ) represents the stretching of the quinoid ring and the lower one ( $\sim 1500 \text{ cm}^{-1}$ ) represents the stretching of the benzenoid ring.<sup>36</sup> The simultaneous presence of the bands in neutral PDPA and in the composites (Figs. 2, 3) informs us that neutral PDPA and the composites possess both amine and imine units. Hence, PDPA exists in polaronic form (Scheme 1). However, there are variations in the intensities of benzenoid and quinoid bands between the composites prepared by the two methods. This indicates that amine/imine sites in PDPA interact differently with sites in MWNT while forming composites through intimate mixing or *in situ* polymerization. It is clear that the intensity of the peak at around  $\sim 1600 \text{ cm}^{-1}$  increases on making a composite by *in situ* polymerization. Otherwise, the imine proportion in the PDPA structure increases when producing a composite through *in situ* polymerization. Hence, we presume that MWNT induces doping in PDPA during *in situ* polymerization. It is important to note that such induced doping should change the absorption band at

around 1170  $\text{cm}^{-1}$ , corresponding to the diphenoquinoneamino imine (Scheme 1) structure. Clearly, the intensity of the band at around 1170  $\text{cm}^{-1}$  increases in the composite (IP1N). Further evidence for the induced doping of PDPA by MWNT was obtained by comparing the FTIR spectra of protonic acid doped PDPA composite (Fig. 3) and neutral composite (Fig. 2). The induction of a positive charge on the nitrogen atom on the macromolecular chain can increase the dipole moment and thus can increase the intensity of the band at around 1170  $\text{cm}^{-1}$ . This is supporting evidence that MWNT induces doping of PDPA. A similar kind of doping was reported for a PANI–fullerene composite.<sup>37</sup>

The FTIR spectra of the composites prepared by intimate mixing (Fig. 2) show the presence of a band at around 1600 and 1500  $\text{cm}^{-1}$ , similar to neutral PDPA. There are only mild variations in the intensities of other bands in comparison to neutral PDPA. This reveals that MWNTs do not induce doping for PDPA as noted for the composite prepared by *in situ* polymerization. The composite prepared from intimate mixing is therefore considered as CNTs wrapped with PDPA. The variations in the positions and intensities of the bands corresponding to C—H in-plane bonding deformation of benzenoid quinoid rings and bending vibrations of C—H (out of plane) demonstrate that newer covalent C—N bands can be formed by the interaction between the imine nitrogen of the repeat units of PDPA and the carbon atoms of MWNTs. Alternatively, there can be formation of C—N coordinate covalent bonds between the polymer chain and radical cation CNT fragments that leads to formation of polymer functionalized CNTs (Scheme 2).

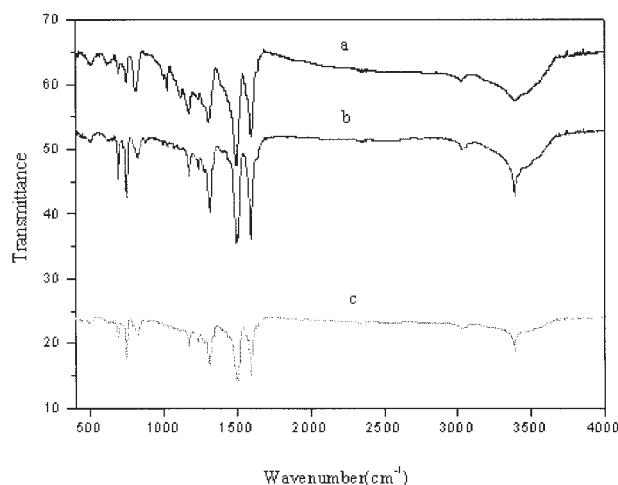
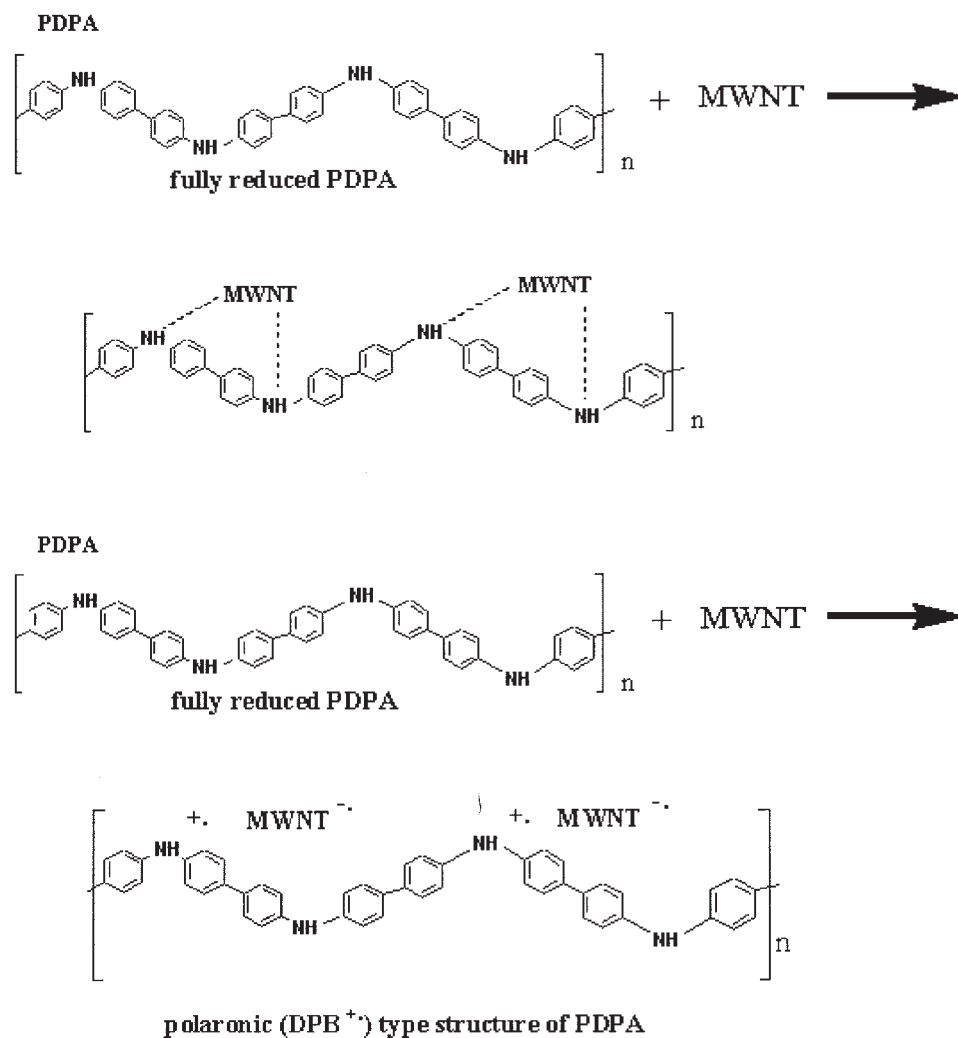


**Figure 3** FTIR spectra of doped composites prepared by *in situ* polymerization: IP1 (spectrum a) and IP2 (spectrum b).



**Scheme 2** Representations of the molecular interactions between PDPA and MWNT: (top) doping-type interactions in the composite prepared by *in situ* polymerization and (bottom) C—N coordinate bond formation resulting in PDPA functionalized MWNT in the composite prepared by intimate mixing.

### Morphology and conductivity

When comparing the SEM images (Fig. 4) of pure MWNT and the composites (Fig. 4), there is a random increase in the diameter of the MWNTs as a result of composite formation. PDPA appears as snowflakes on the tree-branch-like surface of the MWNTs. Few nanoscale defects and scratches in MWNT are seen in the SEM photographs of the composites. We also observed the morphological changes through TEM micrographs. These images (Fig. 5) of PDPA and the MWNT–PDPA composites also supported the morphological variations between the MWNTs and the composites. The periphery of the MWNT became non-uniform after composite formation [Fig. 5(c,d)]. The diameter of the tubular structure for the composite was 10–20 nm higher than the diameter of pure MWNT [Fig. 5(a)]. Part of the PDPA appears as protrusions from the outer walls of the MWNTs in the case of IP1N [Fig. 5(c), inset]. In contrast, the PDPA

appears as finely dispersed particles in the composite prepared by IM1. The protrusions of PDPA or nonuniform dispersion of PDPA appear as defects sites in the MWNTs.

We presume that the conditions used for the preparation of the composites may be the source of the nanoscale defects noticed in the composites. For example, when making the composite by intimate mixing, the mixture of PDPA and MWNT was stirred for a long enough period to attain proper dispersion of the PDPA into the MWNT bundles. This might cause nanoscale defects in the MWNTs. Because of the small size of these defects, they are difficult to repair or control during the synthesis. There are remedial measures that could possibly minimize these defects. For effective healing or minimization of these repairs, Tyagi et al. suggested that the nanotubes can be coated with a polymer that contains nanoparticles.<sup>38</sup> The nanoparticles can potentially migrate to and fill the

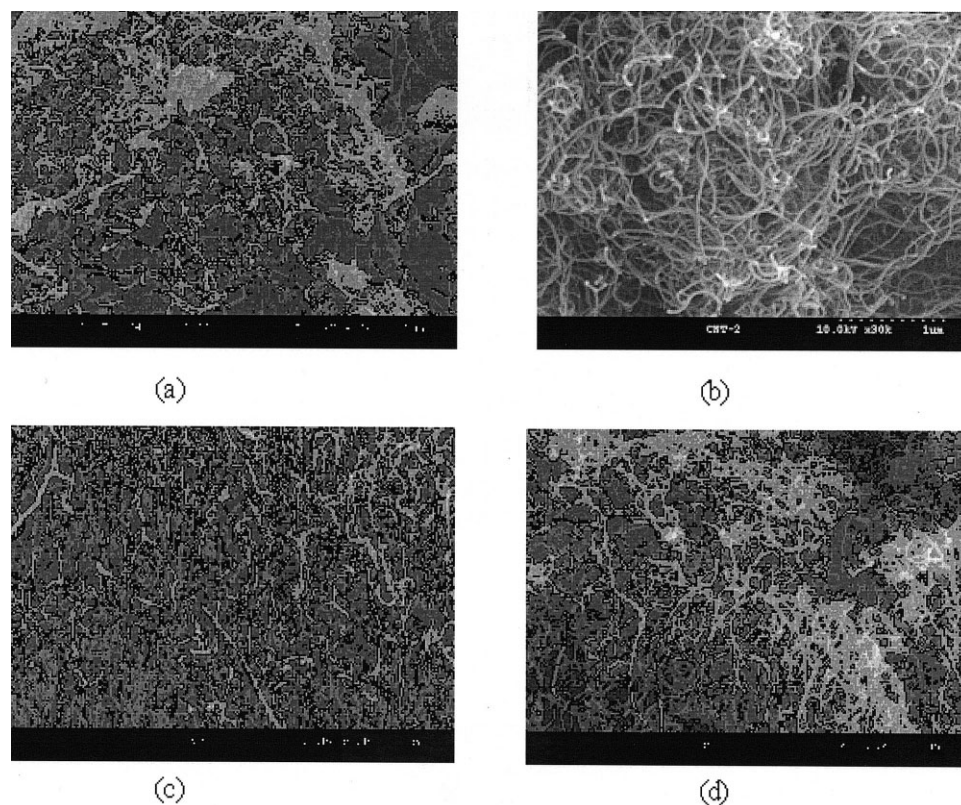


**Figure 4** The SEM morphology of (a) the composite prepared by intimate mixing (IM1N), (b) the composite prepared by *in situ* polymerization (IP1N), (c) neutral PDPA, and (d) pure MWNT.

nanoscopic scratches or voids. Alternatively, the composite of nanotubes may be prepared with a polymer grafted from the nanotube. This approach may provide close proximity of the polymer with the defects in the nanotube. The conductivity values of the composites ( $\sim 10^{-2}$  S/cm) were found to be slightly higher than PDPA ( $\sim 10^{-3}$  S/cm).

### UV-visible spectroscopy

The UV-visible spectra of the composites prepared by intimate mixing (Fig. 6) and *in situ* polymerization (Fig. 7) reveal the differences in the molecular interactions between the components of the composites. Note that the redox state of PDPA in the composites prepared by intimate mixing and *in situ* polymerization may be different. This may be attributable to the differences in the molecular level interactions between the composites prepared by the two methods. In the case of intimate mixing, the formation of C—N coordinate bonding (Scheme 2, top) is not expected to change the electronic state of PDPA. This is clearly evident in the spectra of the composite prepared by intimate mixing. There is no variation in the position of the band at around 320 nm corresponding to the  $\pi$ — $\pi^*$  transition of the neutral form of PDPA.<sup>22</sup> The electronic spectrum of neutral PDPA is presented in the

inset of Figure 6 for comparison. Thus, the electronic state of PDPA is not influenced much in the composite prepared by intimate mixing. Conversely, the electronic spectra of composites IP1 and IP2 show a band at around 570 nm and inform that PDPA is present in the diphenosemiquinoaminoimine (polaronic,  $\text{DPB}^{+\cdot}$ ) form<sup>23</sup> that is due to the probable doping by MWNT (Scheme 2, bottom). This assignment is based on earlier reports on the doping of PANI with acids.<sup>39,40</sup> PANI in the less doped emeraldine base form exhibited a peak at around 620 nm, corresponding to a localized molecular excitonic transition with the electron on a quinoid moiety and a hole on the neighboring moiety. Upon acid induced doping of the emeraldine base to result in an emeraldine salt, the excitonic transition shifted to 580 nm.<sup>39,40</sup> With more MWNTs in the composite, we envision an increase in the probable carboxyl groups generated in the MWNTs during oxidative polymerization with ammonium peroxydisulfate, which might result in more induced doping to PDPA. For a comparison, the electronic spectra of doped PDPA are presented in the inset of Figure 7. Further, composites prepared by *in situ* polymerization with different amounts of MWNTs showed shifting in the band at around 570 nm, corresponding to the oxidized PDPA (polaronic form, Scheme 1). This

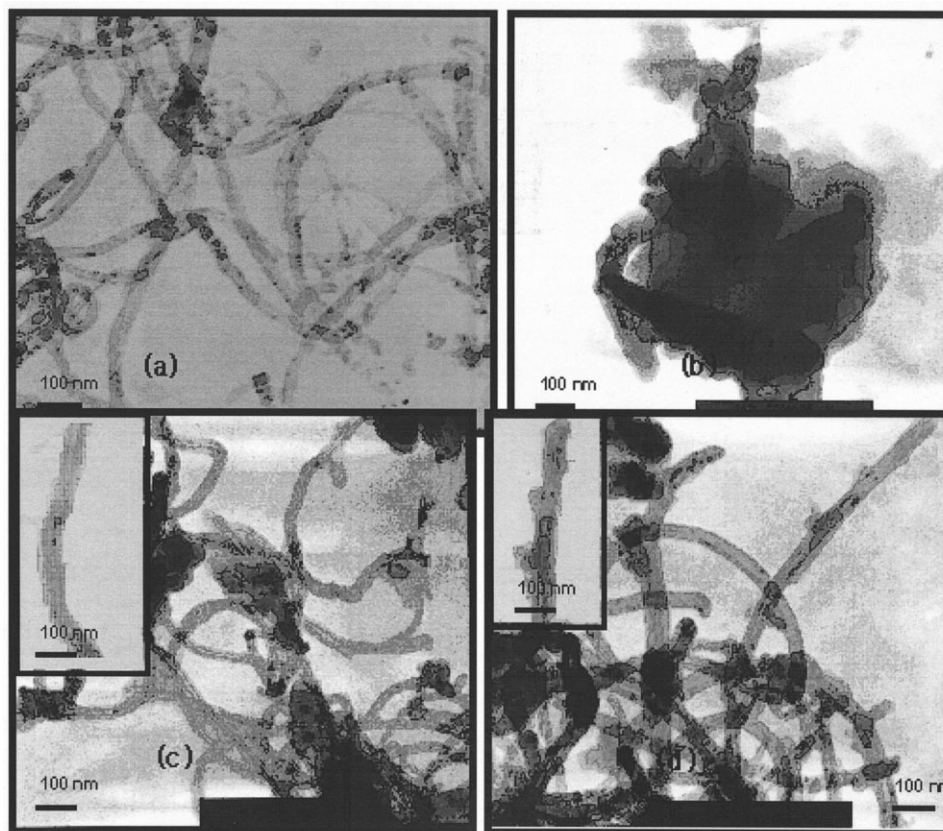


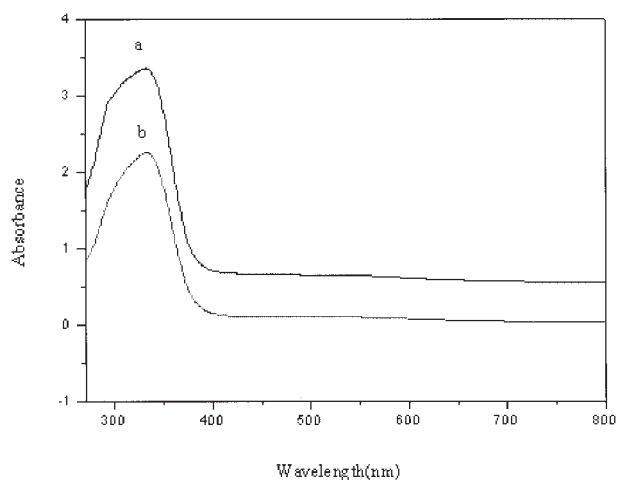
**Figure 5** The TEM morphology of (a) pure MWNT, (b) neutral PDPA, (c) the composite prepared by intimate mixing (IM1N), and (d) the composite prepared by *in situ* polymerization (IP1N).

clearly supports the fact that MWNT induces doping in PDPA.

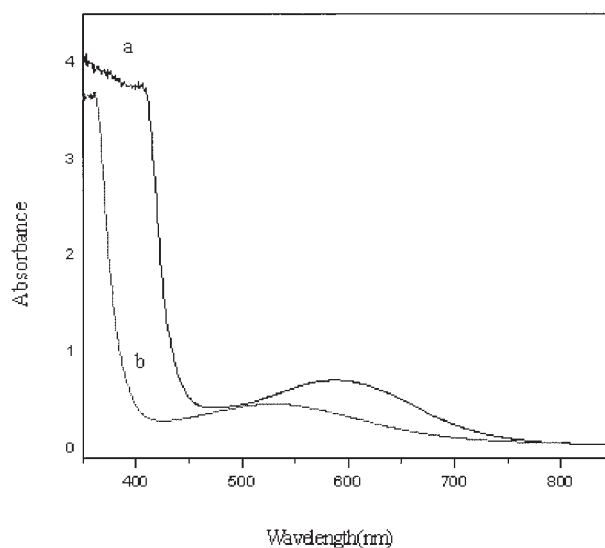
### Thermogravimetric analysis

Figure 8 contains thermograms of the composites prepared by intimate mixing (Fig. 8, curve b) and *in situ*

polymerization (Fig. 8, curve c) in the neutral state. The thermogram of the neutral form of PDPA is also presented (Fig. 8, curve a) for comparison. Note that intimate mixing involves neutral PDPA for mixing



**Figure 6** UV-visible absorption spectra of composites (in DMF) prepared by *in situ* polymerization with different amounts of MWNTs: IP1 (spectrum a) and IP2 (spectrum b).



**Figure 7** UV-visible absorption spectra of composites (in DMF) prepared by intimate mixing: IM1 (spectrum a) and IM2 (spectrum b).

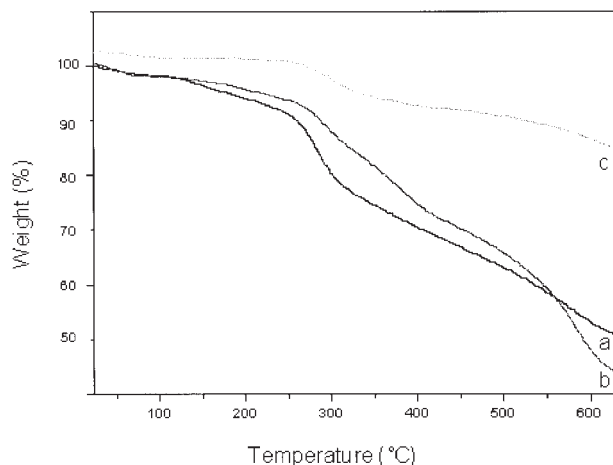


**Figure 8** Thermograms of neutral PDPA (curve a), IP1N (curve b), and IM1N (curve c).

with MWNT and thus results in a neutral composite. By contrast, the doped PDPA generated from *in situ* polymerization makes the composite have PDPA in the doped state. Hence, the composite from *in situ* polymerization was subjected to neutralization to attain the composite in the neutral state (IP1N). Otherwise, in the composites from *in situ* polymerization, the external dopant was specifically removed through neutralization to make the neutral composite, IP1N. The thermogram of neutral PDPA (Fig. 8, curve a) shows two major weight losses corresponding to the loss of water (around 80°C) and decomposition of the backbone structure of PDPA (beyond 300°C). However, the backbone structure of the PDPA in the composites (IP1N and IM1) decomposed at a much higher temperature (>340°C). The existence of molecular level interactions between MWNT and PDPA that is evident from the Raman and FTIR spectra of the composites may be considered as the reason for the improved thermal stability of PDPA units in the composite. IP1N shows a higher extent of weight loss<sup>41</sup> than IM1 beyond 340°C, indicating the presence of more PDPA in IP1N (26%) than in IM1N (87%). The TEM micrograph of IP1N has a number of protruding portions of PDPA [Fig. 5(d)] in IP1N, and that can be considered as the source for the larger amount of PDPA in IP1N than in IM1.

The thermograms of the doped composite prepared by *in situ* polymerization (IP1 and IP2) are also compared with doped PDPA (Fig. 9). The sulfate ions used in the medium of polymerization exist as dopant ions. The weight loss corresponding to the removal of dopant ions takes place well below 300°C. Here again, the weight loss corresponding to the backbone units of PDPA in the composite occurs at a higher temperature (Fig. 9, curves a,b) in comparison to doped PDPA (Fig. 9, curve c). This is also in accordance with the molecular level interactions between MWNTs and PDPA.

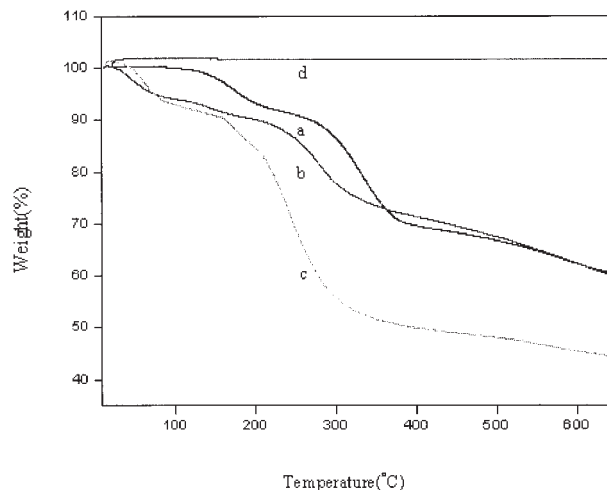


**Figure 9** Thermograms of PDPA/MWNT composites prepared by *in situ* polymerization: IP1 (curve a), IP2 (curve b), doped PDPA (curve c), and pure MWNT (curve d).

#### XRD analysis

The structural characteristics of PDPA/MWNT composites were analyzed by XRD measurements. Figure 10 exhibits the XRD patterns for pure MWNT, PDPA (neutral), and the composites (IP1N, IP2N, and IM1). A comparison of the XRD patterns of the composites with one of their constituents (MWNT or PDPA) infers that there are differences in the structural order between the composites prepared by the two methods. The XRD patterns of IM1 resemble PDPA and the peaks representing the MWNTs (25.7°, 42.8°, and 53.3°). In contrast, composites IP1N and IP2N show a different structural order than IM1. Besides the XRD patterns of MWNT (peaks at 25.8° and 43.0°), additional structural order can be seen through the appear-

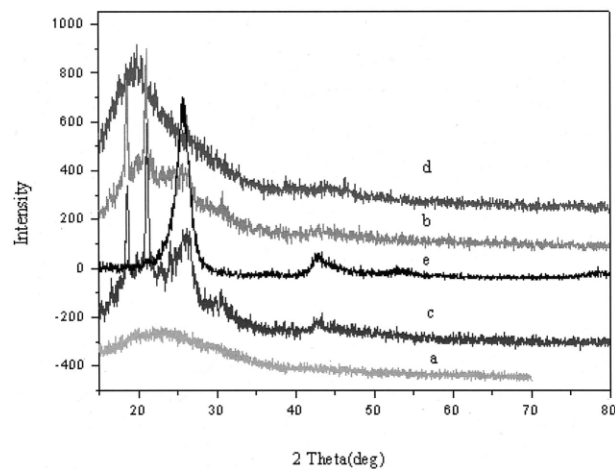


**Figure 10** XRD patterns of the composite prepared by intimate mixing (IM1, spectrum a), the composite prepared by *in situ* polymerization (IP1N, spectrum b), IP2N (spectrum c), neutral PDPA (spectrum d), and pure MWNT (spectrum e).



ance of peaks at 18.5° and 20.9° (due to the presence of PDPA). This type of induction of additional structural ordering was witnessed in composites of MWNT with other polymers.<sup>42–44</sup> Of interest, the peaks at 18.5° and 20.9° were not present in the XRD of neutral PDPA (Fig. 10, curve d). The additional structural order or crystalline domain is expected to originate from the more planar structure adapted for PDPA from the hexagonal surface lattice of the MWNT during *in situ* polymerization.<sup>45</sup> This may arise from strong  $\pi$ – $\pi^*$  interactions between PDPA and MWNT. In addition to the  $\pi$ – $\pi^*$  interaction, other possibilities like charge transfer from PDPA chains and MWNTs through highly reactive imine sites<sup>46,47</sup> may also contribute to the structural order found in this investigation.

### CONCLUSIONS

Composites of PDPA with MWNT were prepared through *in situ* polymerization and intimate mixing of PDPA and MWNT. These composites had different molecular level interactions between the components. Raman and FTIR spectral results revealed that MWNT induced doping in PDPA during *in situ* polymerization. In contrast, a polymer functionalized CNT resulted from the intimate mixing method. These structural differences ultimately influenced the electronic and thermal properties. Comprehensive knowledge on the properties of the prepared nanocomposites would help in deciding the conditions for making composites for desired applications.

The financial support from the Korean Research Foundation is gratefully acknowledged. The authors acknowledge the help of the centre for the high volt transmission microscope at the Korea Basic Science Institute (Daejeon, Korea) for recording the TEM photographs.

### References

- Mintmire, J. W.; Dunlap, B. I.; White, C. T. *Phys Rev Lett* 1992, 68, 631.
- Overney, G.; Zhong, W.; Tomanek, D. Z. *Phys D* 1993, 27, 93.
- Iijima, S.; Ichihashi, T. *Nature* 1993, 363, 603.
- Wong, E. W.; Sheehan, P. E.; Liebe, C. M. *Science* 1997, 277, 1975.
- Schadler, L. S.; Giannaris, S. C.; Ajayan, P. M. *Phys Lett* 1998, 73, 3842.
- Frank, S.; Poncharal, P.; Wang, Z. L.; Heer, W. A. *Science* 1998, 290, 1744.
- Jans, S. J.; Verschueren, A. R. M.; Dekker, C. *Nature* 1998, 393, 49.
- Dai, H.; Hafner, J. H.; Rinzler, A. G.; Colbert, D. T.; Smalley, R. E. *Nature* 1996, 384, 147.
- Tang, B. Z.; Xu, H. Y. *Macromolecules* 1999, 32, 2569.
- Curran, S. A.; Ajayan, P. M.; Blau, W. J.; Carroll, D. L.; Coleman, J. N.; Dalton, A. B.; Davey, A. P.; Drury, A.; McCarthy, B.; Maier, S.; Stevens, A. *Adv Mater* 1998, 10, 1091.
- Ago, H.; Petritsch, H. K.; Shaffer, M. S. P.; Windle, A. H.; Friend, R. H. *Adv Mater* 1999, 11, 1281.
- Musa, I.; Baxendale, M.; Amaratunga, G. A. J.; Eccleston, W. *Synth Met* 1999, 102, 1250.
- Sun, X. H.; Li, C. P.; Wong, N. B.; Lee, C. S.; Lee, S. T.; Teo, B. K. *J Am Chem Soc* 2002, 124, 14464.
- Skotheim, T. A.; Elsenbaumer, R. L.; Reynolds, J. R. *Handbook of Conducting Polymers*; Marcel Dekker: New York, 1997.
- Premamoy, G.; Samir, K. S.; Amit, C. *Eur Polym J* 1999, 35, 699.
- Hassanien, A.; Gao, M.; Tokumoto, M.; Dai, L. *Chem Phys Lett* 2001, 342, 479.
- Deng, J.; Ding, X.; Zhang, W.; Peng, Y.; Wang, J.; Long, X.; Albert, L. P.; Chan, A. S. C. *Eur Polym J* 2002, 38, 2497.
- Maser, W. K.; Benito, A. M.; Callejas, M. A.; Seeger, T.; Martinez, M. T.; Schreiber, J.; Muszynski, J.; Chauvet, O.; Osvath, Z.; Koos, A. A.; Biro, L. P. *Mater Sci Eng C* 2003, 23, 87.
- Yupeng, G.; Kaifeng, Y.; Zichen, W.; Hongding, X. *Carbon* 2002, 41, 1645.
- Feng, W.; Bai, X. D.; Lian, Y. Q.; Liang, J.; Wang, X. G.; Yoshono, K. *Carbon* 2003, 41, 1551.
- Inzelt, G. *J Solid State Electrochem* 2002, 6, 265.
- Chung, C. Y.; Wen, T. C.; Gopalan, A. *Electrochim Acta* 2001, 47, 423.
- Qun, X.; Chun, X.; Qingjiang, W.; Kazuhiko, T.; Hiroshi, T.; Wen, Z.; Litong, J. *J Chromatogr A* 2003, 997, 65.
- Xu, Q.; Zhang, S.; Zhang, W.; Jin, L.; Tanaka, K.; Haraguchi, H.; Itoh, A. *J Anal Chem* 2000, 367, 241.
- Habib, B. M. *J Chromatogr A* 2003, 986, 111.
- Athawale, A.; Milind, V.; Kulkarni, A. *Sens Actuators B* 2000, 67, 173.
- Pagès, H.; Topart, P.; Lemordant, D. *Electrochim Acta* 2001, 46, 2137.
- Santana, H. D.; Dias, F. C. *Mater Chem Phys* 2003, 82, 882.
- Tasi, Y. T.; Wen, T. C.; Gopalan, A. *Sens Actuators B* 2003, 96, 646.
- Wen, T. C.; Chen, J. B.; Gopalan, A. *Mater Lett* 2002, 57, 280.
- Hua, F.; Ruckenstein, E. *Langmuir* 2004, 20, 3954.
- Hua, F.; Ruckenstein, E. *Macromolecules* 2003, 36, 9971.
- Cochet, M.; Maser, W. K.; Benito, A. M.; Callijas, M. A.; Martinez, M. T.; Benoit, J. M.; Schreiber, J.; Chauvet, O. *Chem Commun* 2001, 16, 1450.
- Baibarc, M.; Baltog, I.; Lefrant, S.; Mevellec, J. Y.; Chauvet, O. *Chem Mater* 2003, 15, 4149.
- Dresselhauss, M. S.; Dresselhauss, G.; Eklurd, P. C. *Fullerenes and Carbon Nanotubes*; Academic: New York, 1996.
- Huang, L. M.; Wen, T. C.; Gopalan, A. *Mater Lett* 2003, 57, 1765.
- Glusca, M.; Baibarac, M.; Lefrant, S.; Chauvet, O.; Baltog, I.; Devenyi, A.; Manila, R. *Carbon* 2002, 40, 1565.
- Tyagi, S.; Lee, J. Y.; Buxton, G. A.; Balazs, A. C. *Macromolecules* 2004, 27, 9160.
- Duke, C. B.; Conwell, E. M.; Paton, A. *Chem Phys Lett* 1986, 131, 82.
- Tzou, K.; Gregory, R. V. *Synth Met* 1993, 53, 365.
- Wu, M. S.; Wen, T. C.; Gopalan, A. *Mater Chem Phys* 2002, 74, 58.
- Chang, T. E.; Jensen, L. R.; Kisliuk, A.; Pipes, R. B.; Pyrz, R.; Sokolov, A. P. *Polymer* 2005, 46, 439.
- Zhang, X.; Sreekumar, T. V.; Liu, T.; Kumar, S. *J Phys Chem B* 2004, 108, 16435.
- Assouline, E.; Lustiger, A.; Barber, A. H.; Cooper, C. A.; Klein, E.; Wachtel, E.; Wagner, H. D. *J Polym Sci Part B: Polym Phys* 2003, 41, 520.
- Sainz, R.; Benito, A. N.; Martinez, T.; Galindo, J. F.; Sotres, J.; Baro, A. M.; Corraze, B.; Chauvet, O.; Maser, W. K. *Adv Mater* 2005, 17, 278.
- Cochet, M.; Maser, W. K.; Benito, A. M.; Callejas, M. A.; Martinez, M. T.; Benoit, J. M.; Schreiber, J.; Chauvet, O. *Chem Commun* 2001, 1450.
- Zengin, H.; Zhou, W.; Jin, J.; Czerw, R.; Smith, D. W.; Eche-goyen, K.; Carroll, D. L.; Foulger, S. H.; Ballato, J. *Adv Mater* 2002, 14, 1480.